Journal of Hazardous Materials 163 (2009) 783–794

Contents lists available at ScienceDirect

Journal of Hazardous Materials

journal homepage: www.elsevier.com/locate/jhazmat

Flame acceleration and the development of detonation in fuel–oxygen mixtures at elevated temperatures and pressures

G.O. Thomas*

Combustion Hazard Research, c/o DDtexperts, PO Box 217, Llanerch BronPadarn, Aberystwyth SY23 3XT, UK

ARTICLE INFO

Article history:
Received 28 September 2007
Received in revised form 6 July 2008
Accepted 8 July 2008
Available online 31 July 2008

Keywords:
Detonation limits
Fuel–oxygen
Elevated temperature and pressure

ABSTRACT

Experimental measurements of the conditions required for the development of detonation in a 7 mm tube following ignition by a low energy spark are reported. There are then compared to previous experimental propagation limit criterion using theoretical predictions of detonation cell sizes based on a one-dimensional detonation length scale computed using a detailed chemical kinetic scheme. Technical difficulties precluded direct cell size measurements. Ethylene–oxygen and hydrogen–methane–oxygen mixtures were investigated as well as methane-ammonia-oxygen, at initial pressures and temperatures in the ranges 1–7 bar and 293–540 K, respectively. The likelihood of detonation in ethylene-air mixtures in 150 mm and 50 mm pipes at ambient initial conditions is also discussed in relation to published cell width data.The results indicate that whilst detonation cell width predictions do not provide a quantitative measure of the conditions for which detonation may develop in a pipe of given diameter, for prescribed initial conditions, predicted detonation cell size data does provide useful qualitative guidance as to possible hazardous compositions, particularly if preliminary experimental safety testing is thought to be necessary.

1. Introduction

Detonation is perhaps the most enigmatic of all combustion phenomena, the result of an intricate coupling between gas-dynamics and high temperature exothermic reaction. Propagating detonations exhibit complex three-dimensional structure yet macroscopic detonation properties such as peak pressure and velocity can still be predicted from simple one-dimensional theory. Unfortunately, despite this ability to *compute* these macroscopic properties accurately, the reality is that our ability to *predict* whether a detonation will develop under given initial conditions is far more limited. This inability is of both fundamental and practical concern. The fundamental problems of interest are the coupled time dependent chemical and gasdynamic processes that govern the microscopic characteristics of combustion. The practical interests arise when attempting to assess safe operating conditions for chemical processes.

One important practical concern in chemical plants is whether detonation in a mixture can be *sustained* in a pipe of given diameter. Of equal concern is whether a detonation will actually be *established* following ignition by a low energy source. An approach adopted by previous researchers was to correlate a natural characteristic length scale of detonation at the limit of propagation with the pipe diameter. This analysis was developed for studies with fuel-air mixtures at ambient initial temperature and pressure using an energetic source, either an established detonation or a strong shock wave.

In the present paper observations are presented of flame acceleration and possible transition to detonation in various fuel–oxygen mixtures at ambient and elevated temperatures and pressures. Unlike previous studies of propagation limits a much lower ignition energy source was used, a 0.6J electric spark. Cell sizes estimated from theoretical predictions of auto-ignition delay times were used to investigate further the validity of an *a priori* approach for predicting detonation establishment limits. The cell size predictions were validated wherever possible against existing cell size data. Direct measurements of cell sizes at the present elevated temperatures and pressures were not possible because of the technical difficulties associated with such measurements.

2. Detonation structure and propagation limits

Although thermodynamic calculations are known to provide very accurate predictions of the properties of a detonation wave (pressure, velocity, etc.) such calculations cannot predict whether a given detonation *will* or indeed *can* propagate under certain physical conditions. One reason for this is that a detonation wave is

* Tel.: +44 845 327 3784.
E-mail address: geraint@ddtexperts.com.

0304-3894/$ – see front matter © 2008 Elsevier B.V. All rights reserved.
doi:10.1016/j.jhazmat.2008.07.105

not truly one-dimensional but has a complex three-dimensional shock structure. It is only if this structure can be generated and maintained that steady self-sustaining detonation can evolve.

Classical Chapman-Jouguet (CJ) theory provides an accurate means of predicting detonation wave properties using the one-dimensional conservation equations of mass, energy and momentum together with an appropriate chemical energy release term. CJ theory assumes infinitely fast reaction. Finite rate chemistry was allowed for later in the theory developed by Zeldovitch, von Neuman and Doring, the ZND model. The ZND model allows thermal auto-ignition reactions to be initiated in the high pressure and temperature von Neumann region behind the lead shock. Exothermic reaction thus begins after a finite delay. The lead shock moves at the detonation velocity and the conditions that arise in the CJ theory are now developed at the end of the exothermic reaction zone, and not at a single discontinuity at the leading wavefront.

In the ZND model, shown schematically in Fig. 1, the lead shock S propagates at the CJ detonation velocity D_{cj} and the pressure and temperature in the gas flow immediately behind this shock lead to auto-ignition of the gas, after an appropriate ignition delay τ_i. Exothermic reaction starts at R. In a laboratory frame of reference the velocity U_{vn}, temperature T_{vn} and pressure P_{vn} of the post shock gas can be computed using the velocity D_{cj} in standard shock relations. In a reference frame at rest with respect to the detonation front, knowledge of the shocked velocity gas in the von Neumann spike, V_{vn}, allows the induction zone length L_i to be calculated if τ_i is known, as $L_i = V_{vn}\tau_i$.

In practice an examination of a detonation front reveals large deviations from this one-dimensional image. These are also predicted when linearised stability theory is applied to ZND waves. This form of analysis was pioneered by Erpenbeck [1] and led to the conclusion that in practice most ZND wave profiles are universally unstable to certain transverse wavelengths. More recently studies such as those described by Stewart [2,3] have been developed and refined and allow cellular structure to emerge directly from the solutions. These instabilities are most striking when seen on smoked foil records, where patterns on a pre-treated surface are left by the intersecting transverse shocks. The characteristic patterns formed by these interactions are generally diamond in shape and are termed 'cells'. They are a universal feature of self-sustaining gaseous detonation. The characteristic dimensions of the cell structure are dependant on the chemical system and 'cell' width and length are a function of initial chemical composition, dilution, initial pressure and temperature. It is easy to surmise therefore that variations in the detonability of different mixtures in different geometries might be intimately linked to the initial chemical and physical properties of the mixture. It is this aspect that is explored in the present paper. For more detailed descriptions of detonation theory and structure see Nettleton [4], Strehlow [5] and Edwards et al. [6].

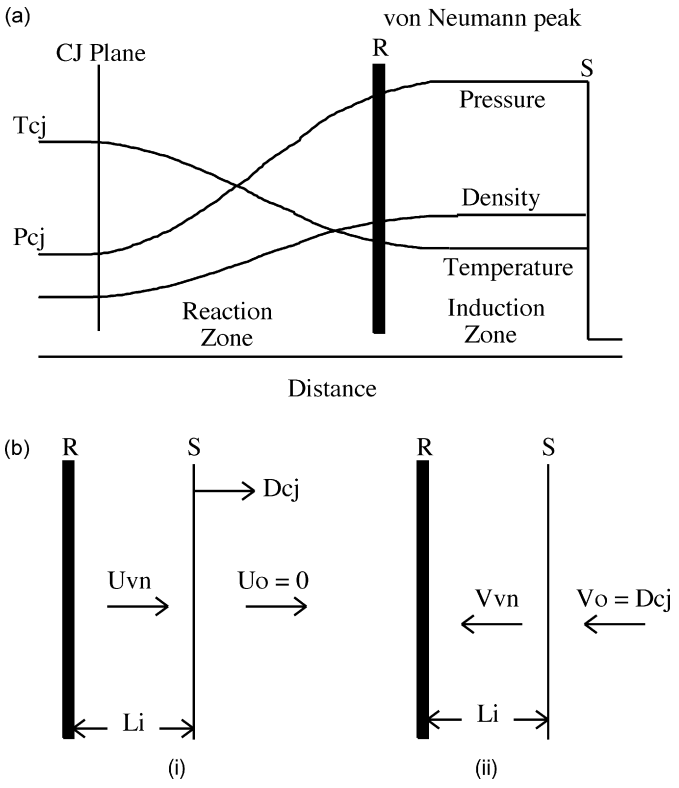

Fig. 1. Schematic illustrating (a) evolution of pressure and temperature in the ZND model of detonation and (b) induction zone length L_i and gas velocities in (i) laboratory and (ii) detonation frame of reference. S—lead shock; R—start of exothermic reaction.

3. Previous studies of detonation limits

The most comprehensive series of studies of detonation propagation limits are those by Dupré et al. In a series of studies, they monitored the propagation of established detonations in fuel-air mixtures through a series of pipes of decreasing diameter until the detonation was observed to fail. In this way, critical pipe diameters could be determined [7,8]. These data, obtained as a function of fuel type and equivalence ratio, were then compared to measured detonation cell sizes. Dupré et al. [7] concluded that detonations could not propagate if the detonation cell width, λ, of a mixture was greater than πD, where D is the pipe diameter. This was greater than the $\lambda = 1.7$ D condition identified previously by Moen et al. [9]. Later studies by Dupré et al. [8] revised the estimate of the critical condition for propagation to $\pi D < \lambda < 2\pi D$, although they recognised $\lambda = D$ as realistic limit criterion because of uncertainties in detonation cell structure near the limit.

Most previous studies of the onset of detonation in fuel–oxygen mixtures on the other hand have been concerned with the transition to detonation distance, the distance from the point at which combustion is first initiated to the point at which detonation starts. A comprehensive set of measurements was reported by Bollinger and co-workers. Bollinger et al. [10,11,12] investigated transition distances in fuel–oxygen mixtures in tubes of internal diameter 15 mm and 50 mm at temperatures of 40 °C with some as high as 200 °C. The internal surfaces were honed to a mirror finish. The smaller diameter tube was 2.9 m long and the 50 mm diameter was 3.6 m in length. Initial test gas pressures of 1, 5, 10 and 25 atmospheres were tested. The gas mixtures tested were hydrogen-, methane-, carbon- monoxide- and acetylene-oxygen for a range of equivalence ratios. An anticipated increase in transition distance as the mixtures moved away from stoichiometry was observed as was a strong dependence on initial pressure. Ginsburgh and Bulkley [13] also report some data on the positive influence of initial pressure in reducing the transition to detonation distance in ethylene–oxygen with 52% N_2 dilution mixtures in a 50 mm diameter pipe. Popov [14] reported flame acceleration and DDT in a 3 m long 20 mm pipe with stoichiometric hydrogen-oxygen. In a related study, the influence of temperature on flammability limits was investigated by Bunev [15] for methanol- and hydrogen-air for temperatures up to 720 K. The found that at temperatures in excess of 500 K residence time was an important factor, due to the influence of oxidising reactions. More recently Shebko et al. [16] studied the flammability of hydrogen-air at up to 525 K and 40bar. In common with many other studies

this high pressure work was concerned mainly with stoichiometric mixtures and less attention has been given to limits as a function of concentration. Chapin et al. [17] later studied deflagration to detonation transition (DDT) in hydrogen-air mixtures and determined the effect of initial gas velocity in a 50 mm diameter tube in addition to the influence of increasing temperature and pressure, up to 615 K and 4 bar, respectively.

DDT studies in an obstacle laden 100 mm diameter tube with hydrogen-, acetylene-, ethylene- or JP10- air mixtures at temperatures up to 573 K and a maximum pressure of 2 bar were reported recently by Card et al. [18] who found a correlation between measured detonation cell size and a critical obstacle dimension.

The highest pressures studied to date are those reported by Bauer and Presles [19,20] for methane- and ethylene-air, where the initial pressures were as high as 40bar The emphasis in these studies was however more on determining the macroscopic parameters of established detonation waves than the determination of propagation limits.

4. Kinetic predictions of detonation limits

As discussed earlier, three-dimensional detonation structure is manifested as diamond like 'cell' imprints left on a lightly sooted surface. The characteristic sizes of the cells are related to the chemical reactivity of the system and they increase in size as the reactivity or the initial pressure decrease. Dupré et al. [7,8] used this property to estimate propagation limits in circular tube and found that mixtures with measured 'cell' widths λ greater than $2\pi D$ could not sustain detonation.

It has been suggested by several authors that correlations between chemical kinetics, induction zone length and cell size may be possible. Belles [21] investigated the kinetic requirements for hydrogen explosions and obtained good agreement for detonation limits predicted from low-temperature explosion limit studies. Westbrook and Urtiew [22,23] used a detailed kinetic scheme for a range of fuels and found correlations between various limit parameters and induction zone length.

Detonation cell lengths may also be estimated as simple multiples of induction zone lengths, and values of the order 60–120 were reported by Strehlow and Engel [24,25]. Also the ratio of cell width to cell length is usually of the order of 0.6, see Bull et al. [26] and Strehlow and Engel [25]. Therefore, if the von Neumann pressure and temperatures are known, together with an appropriate chemical kinetic reaction scheme, the auto-ignition delay time τ_i and induction zone length L_i can be estimated. Hence the cell width, λ, can be computed using $\lambda = nL_i$ where n is an arbitrary constant of order 35–75. More recent examples of the application of this approach are those reported by Bradley [27], Gavrikov et al. [28] and Auffret et al. [29] The latter studied acetylene-oxygen mixtures and found good agreement between predicted detonation cell dimensions and experimental data. Agafonov and Frolov [30] on the other hand computed limit parameters for hydrogen-oxygen mixtures using an analytical approach to combine the conservation equations for mass, energy and momentum with a detailed chemical kinetics scheme. Ng et al. [31] were also concerned with hydrogen-air hazards and used chemical kinetic predictions to assess possible detonation hazards.

During the course of the present work we have estimated cell size widths from kinetic based estimates of auto-ignition delays and induction zone lengths in the idealised von Neumann peak. The detonation properties of the mixtures were first computed using the NASA thermodynamic equilibrium code. This gives accurate predictions of CJ detonation velocity, pressure and temperature. Using the computed CJ detonation velocity, the gasdynamic and thermodynamic states in the post shock von Neumann region were

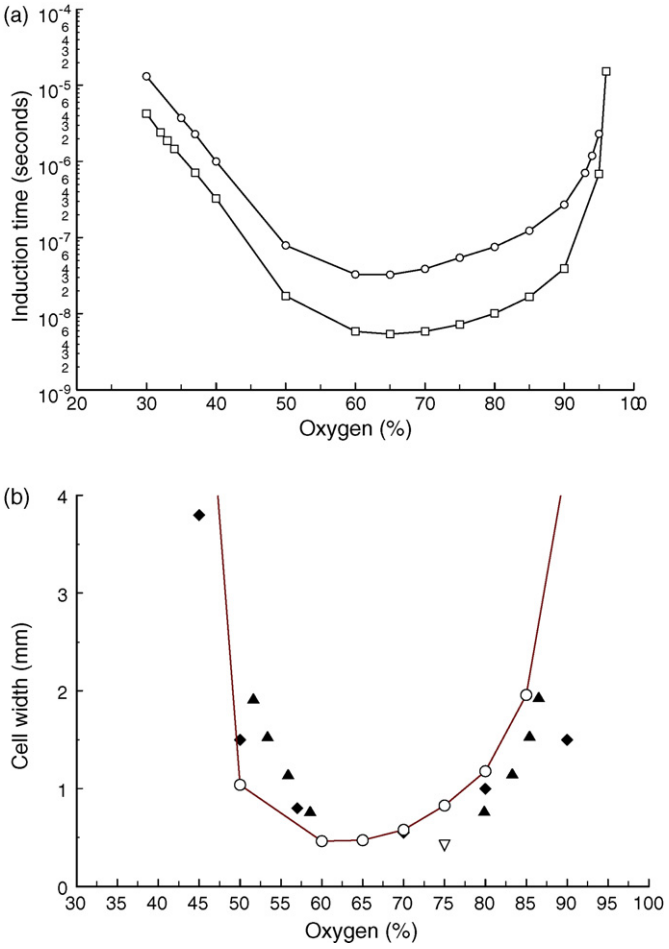

Fig. 2. (a) Computed auto-ignition delay times for ethylene–oxygen as a function of oxygen content. Initial pressure 1 bar - ○, 7 bar -□. Initial temperature 293 K. (b) Plots of cell widths as a function of oxygen percentage in ethylene–oxygen. Initial temperature 293 K, pressure 1 bar. Present kinetic predictions—○, Bradley measured - ♦, Makris [28] measured $D_{crit}/13$ -▲, Strehlow [22,23] measured extrapolated -▼.

then computed using the DSHOCK routines provided as part of the SANDIA suite of CHEMKIN packages. This package was also used to integrate chemical kinetic rate equation schemes. The auto-ignition delay time was determined by monitoring temperature. The kinetic scheme used for most calculations was that give by Tan [32].

Ignition delay times computed in this manner for ethylene–oxygen mixtures for a range of oxygen concentrations are shown in Fig. 2(a). Here the delays have been computed at an initial temperature of 293 K for two initial pressures, 1 bar and 7 bar. Similar calculations were made at an initial temperature of 540 K, again at initial pressures of 1 bar and 7 bar. In this instance the value used for the constant n relating λ and τ_i was 60. A comparison of the predicted variation in detonation cell width with oxygen concentration at 1 bar and 293 K is plotted in Fig. 2(b). These data are plotted together with previous measurements or estimates of cell width. From Fig. 2(b) it can be seen that the predicted cell widths are in reasonable agreement with those measured by Bradley [27], a point extrapolated from measurements at lower initial pressures after Strehlow and Engel [24,25] and cell widths and estimates by Makris et al. [33] based on the critical diameter, D_{crit}. The latter measurement is commonly used to characterise the detonability of atmospheric fuel-air mixtures, see for example Moen et al. [34], and investigations have shown that D_{crit} is close to thirteen times the cell width for many mixtures.

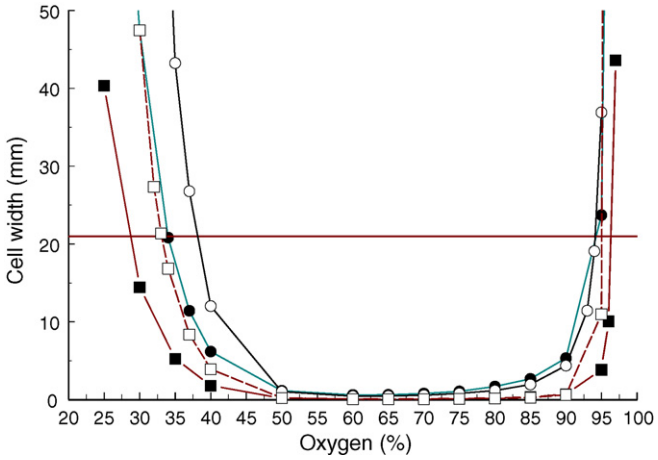

Fig. 3. Predicted cell widths based on auto-ignition delay times at von Neumann temperatures and pressures. Initial pressure 1 bar, initial temperatures 293 K -○, 540 K - ●. Initial pressure 7 bar, initial temperature 293 K -□, 540K - ■.

The predicted cell widths for initial pressures of 1 and 7 bar and initial temperatures 293 and 540 K are plotted on Fig. 3 as a function of oxygen content.

5. Experimental details

The experiments were conducted in 1.48 m long 7 mm internal diameter stainless steel tube, wall thickness 2.5 mm. The tube, shown schematically in Fig. 4, could be heated using standard heating tape and insulated using Kaowool. The initial temperatures used during the present study were 293 K, 393 K and 540 K. The gas pressure was regulated by a needle valve located a short distance after the end of the test section, used in conjunction with a mass flow controller. Initial gas pressures were monitored using a general purpose pressure gauge, 10 bar full scale. Two initial gas pressures were used, 1 bar and 7 bar.

Transient pressures at ambient initial temperatures were monitored using a PCB pressure gauge. Pressure measurements at higher initial temperatures were measured using a high temperature Kistler gauge. Type K thermocouples, diameter 0.5 mm, were used to monitor the gas temperature, mounted such that their tips were located close to the centre line of the tube. The thermocouples monitored the initial gas temperature as well as detecting hot combustion products. Given the thermocouple rise times it was possible to monitor flame propagation by observing the onset of temperature increases. The response times were not sufficient however to record the true transient temperatures.

Gas composition and flow rates were set using an MKS three channel mass flow controller and display unit. Variations in test gas compositions were obtained by adjusting the relative mass flow rates of each component. Ignition of test mixtures was attempted using a short duration spark, nominal energy 0.6 J spark.

6. Experimental results

6.1. Ethylene–oxygen

Tests at ambient initial temperature (293 K) and pressure (1 bar) were conducted over a wide range of stoichiometries. Typical pressure histories obtained from the PCB gauge are reproduced in Fig. 5 (a–d). The lowest concentration it proved possible to ignite at ambient initial pressure with the present arrangement was 40% oxygen and the pressure record obtained is characteristic of a slow oscillating flame, see Fig. 5(a). With an increase in oxygen concentration, to 43%, a peak pressure of *ca.* 1.4 bar was observed, Fig. 5(b). A weak shock was formed ahead of a flame at 46% oxygen, Fig. 5(c), whereas an established detonation arrived at the pressure gauge for an oxygen concentration of 48%, as shown in Fig. 5(d). Detonation was then observed in all further tests until the oxygen concentrations reached 92%, beyond which the various pressure histories obtained for fuel rich mixtures were repeated in reverse order. Thus, as the oxygen concentration was increased further beyond 92% the overpressures continued to decrease and the overall duration of the combustion event increased significantly. A summary of peak pressures from these tests is presented in Fig. 6(a). Theoretical values of the CJ pressures predicted for a steady detonation at ambient initial conditions are shown as a solid line.

Also plotted on Fig. 6(a) are the peak pressures obtained with an initial temperature of 393 K. Limits of establishment of detonation

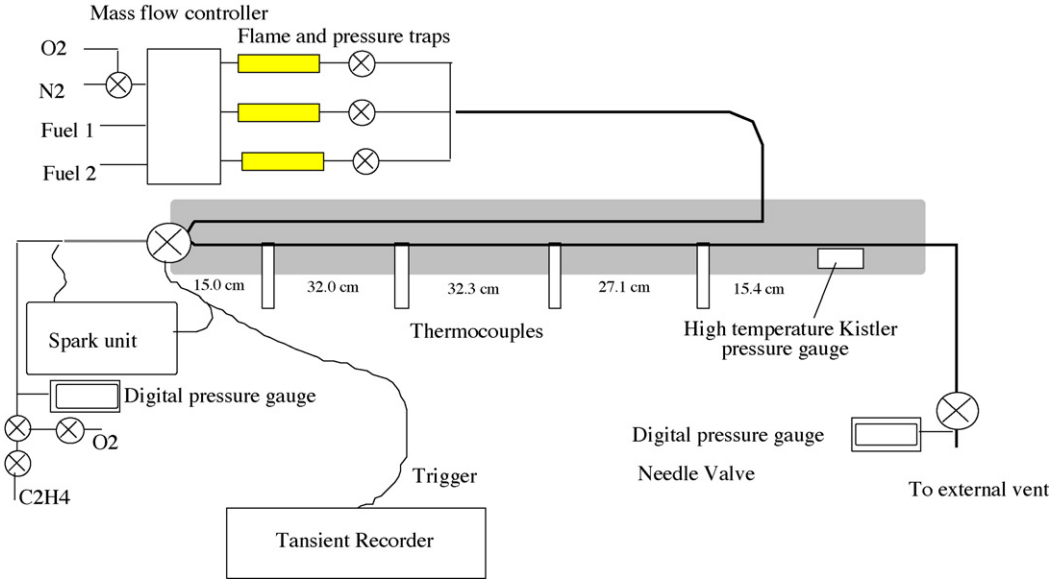

Fig. 4. Schematic drawing of general experimental configuration.

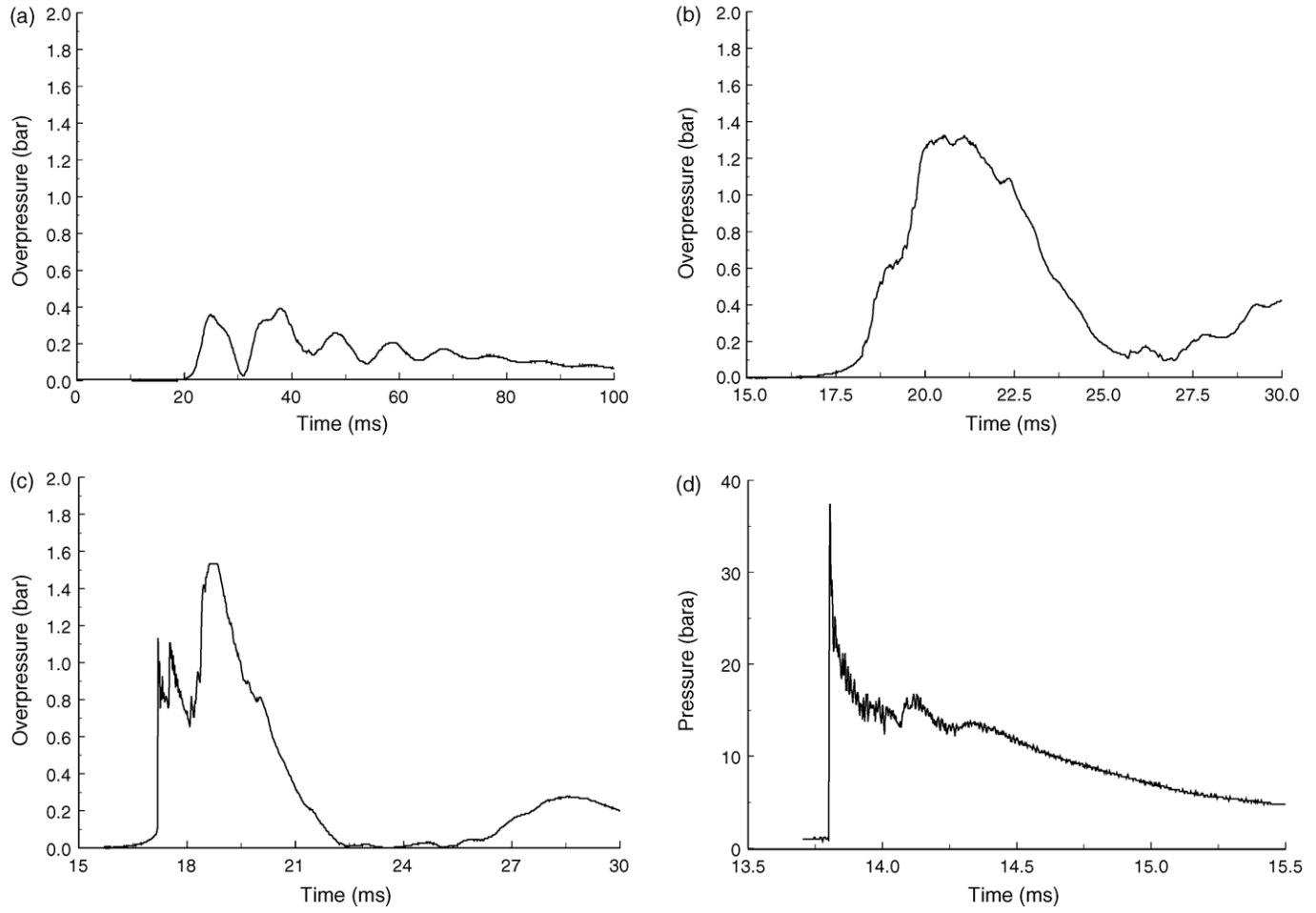

Fig. 5. Representative pressure histories in various ethylene–oxygen compositions in a 1.48 m long 7 mm diameter tube. Pressure gauge at 1.28 m from spark source. Initial pressure 1 bar. Initial temperature 293 K. Oxygen concentration (a) 40%, (b) 43%, (c) 46% and (d) 48%.

can be estimated for both test series. The general character of the pressure records across the mixture composition range from rich to lean was again as observed in the preceding tests. At 393 K and 1 bar, the minimum oxygen concentration that could be ignited was 38% oxygen.

When the initial pressures was increased to 7 bar, at an initial temperature 293 K, the general characteristics of the pressure records again varied with oxygen concentration in a similar manner to that observed in the tests at lower initial pressure. The lowest oxygen composition that could now be ignited was however reduced to 26% oxygen. Detonation was first observed at 35% oxygen. This limit is shown clearly in plots of peak pressure versus oxygen concentration presented in Fig. 6(b). In this case the peak pressures are normalised to the initial pressures.

Two pressure records obtained at initial oxygen compositions of 35% and 36% oxygen in ethylene are presented in Fig. 7(a) and (b), for an initial temperature and pressure of 393 K and 7 bar, respectively. With 35% oxygen in ethylene an oscillatory combustion wave was obtained. The rate of pressure rise indicates rapid flame acceleration but there is no evidence of incipient transition to detonation. At an oxygen concentration of 36%, however, early flame acceleration led to the formation of a pre-cursor shock. Subsequent flame acceleration in this pre-shocked and compressed and heated gas, now at *ca.* 12 bar, leads to a further brief shock compression to *ca.* 20 bar at which point the mixture detonated, giving a peak pressure well in excess of the maximum pressure rating of the Kistler gauges in this temperature range (350 bar). The gauge could no longer be used for any quantitative measurements after this test.

During a further final series of test at an initial temperature of 540 K and pressure of 1 bar the output from the damaged gauge was sufficient to allow detonation to be identified. In this way detonation was observed to have developed at 47% oxygen, but not at 46% oxygen. The limit identified at 540 K is very similar to that obtained in the lower temperature tests at 1 atmosphere initial pressure. When the initial pressure was increased to 7 bar the damaged Kistler gauge provided a pressure output where a pre-cursor shock and subsequent DDT event could be clearly identified, at an oxygen concentration of 35%. Increasing the oxygen composition to 36% gave a clear detonation wave at the gauge. The lean and rich detonation limits identified during the entire test series are summarised in Table 1.

6.2. Methane–hydrogen–oxygen

The primary interest is this series of experiments was the influence of changes in the relative fuel content of binary mixtures. Methane and hydrogen were chosen as they represent extremes of detonability for the fuels commonly used in fuel-air explosion research. The initial pressures and temperatures were 293 K and 1 bar in all cases.

Examples of peak pressures versus oxygen concentration for binary fuel mixtures, 33%H_2 with 67%CH_4 and 33%CH_4 with 67%H_2

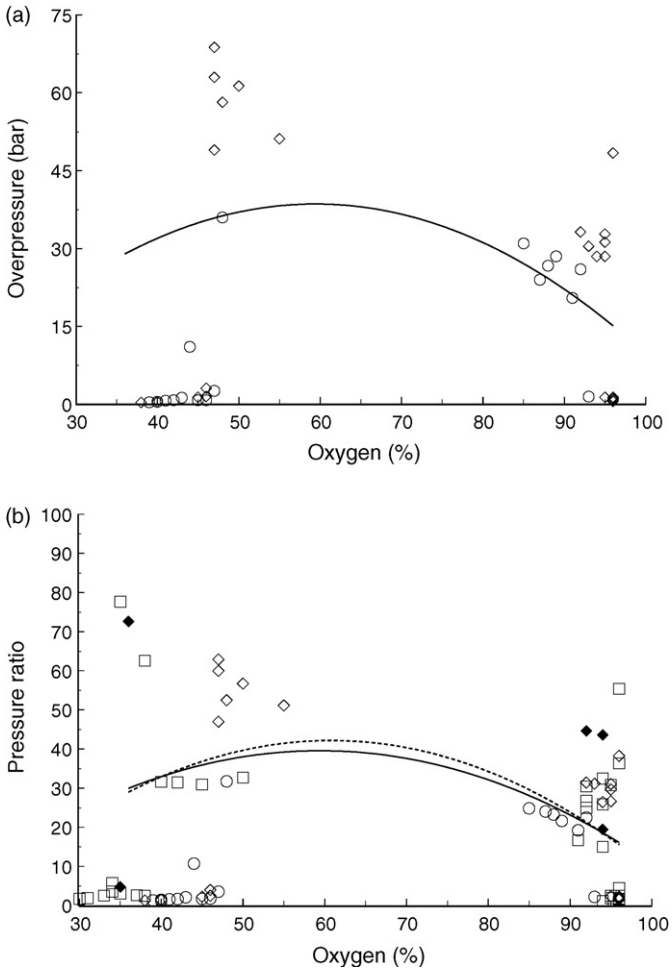

Fig. 6. (a) Peak overpressures as a function of oxygen concentration in ethylene–oxygen: ○- 293 K, 1 bar; ◊ - 393 K, 1 bar. Initial temperature. Initial pressure, 1 bar. Solid line - theoretical CJ pressure 1 bar 293 K; (b) Ratios of peak overpressure to initial pressure as a function of oxygen concentration in ethylene–oxygen: ○- 293 K, 1 bar; ◊ - 393 K, 1 bar; □- 293 K, 7 bar; ♦- 393 K, 7 bar. Lines - theoretical CJ pressure; initial temperature 293 K; Initial pressure, solid - 1 bar, dashed - 7 bar.

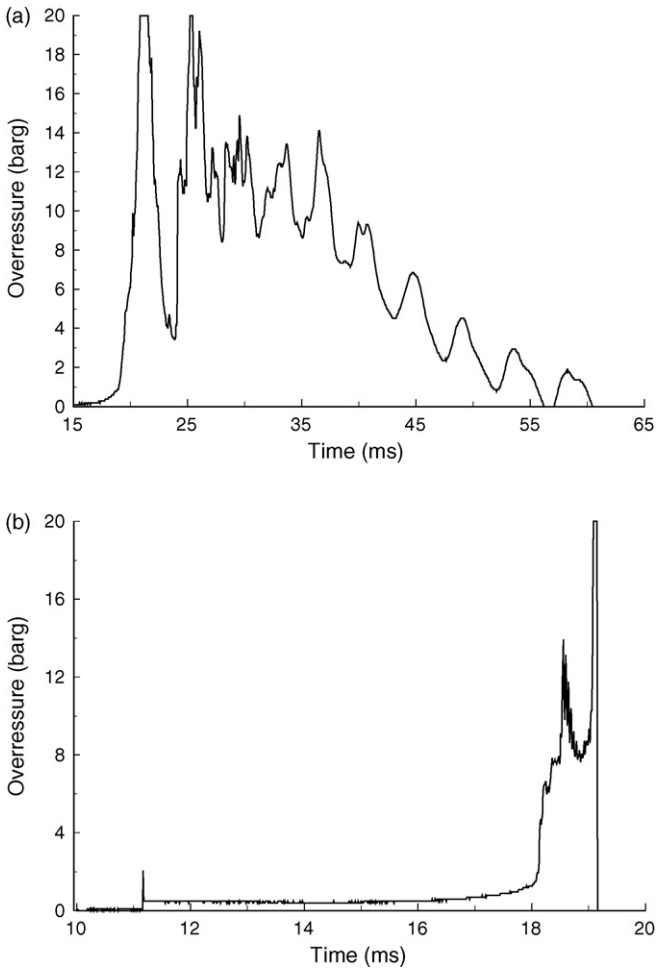

Fig. 7. Representative pressure histories in various ethylene–oxygen compositions in a 1.48 m long 7 mm diameter tube. Pressure gauge at 1.28 m from spark source. Initial pressure 7 bar. Initial temperature 393 K. Oxygen concentration (a) 35%, (b) 36%.

are plotted in Fig. 8(a). The times to peak pressure for these mixtures, as well as for the pure fuels with oxygen, are presented in Fig. 8(b). The variations in dependence on oxygen concentration apparent between these plots is greatly minimised however when the compositions are plotted in terms of their individual fuel equivalence ratios, as shown in Fig. 9(a). For completeness, as different investigators may assume differing definitions for equivalence ratio, this data is also plotted on Fig. 9(b) as a function of fuel/oxygen equivalence ratio. The latter uses the ratio of the fuel/oxygen fraction ratio in the mixture to the value at stoichiometry, as opposed to just using the corresponding ratio of fuel concentration. The two approaches give significant differences for fuel–oxygen or low dilution mixtures. The differences for fuel-air mixtures are less.

Table 1
Summary of upper and lower concentration limits of oxygen in ethylene as a function of initial gas temperature and pressure for which detonation was observed in a 7 mm tube

Temperature (K)	Pressure (Bar)	Upper limit O_2 (%)	Lower limit (%)
293	1	92	48
393	1	95	47
540	1	–	47
293	7	94	38
393	7	94	36
540	7	–	36

Concentration values are accurate to ±1%.

7. Discussion

7.1. Ethylene–oxygen

Previously published values for the limits of detonation propagation are quoted by Wagner [35] and Pusch [36] as 95.8% and 97.7% oxygen for the fuel lean limit and the corresponding values are 40% and 39% for the rich limit. The establishment limits determined in the present study are summarised in Table 1. For mixtures at ambient temperatures and pressures the agreement between the present and previous studies is good at the fuel rich limit but less so at the fuel lean limit, where the limiting oxygen differs by more than 4% from the earlier results.

Fig. 12 present cell size estimates from the present study based on induction zone calculations and, following Strehlow and Engle [24,25], an arbitrary multiplication factor $n = 60$. Also plotted are the cell width measurements of Bradley [25]. The agreement between predictions and measurements is good for oxygen concentrations between 50% and 80% but the predicted cell sizes increase rapidly outside this range. Fig. 10 also contains an indication, by vertical

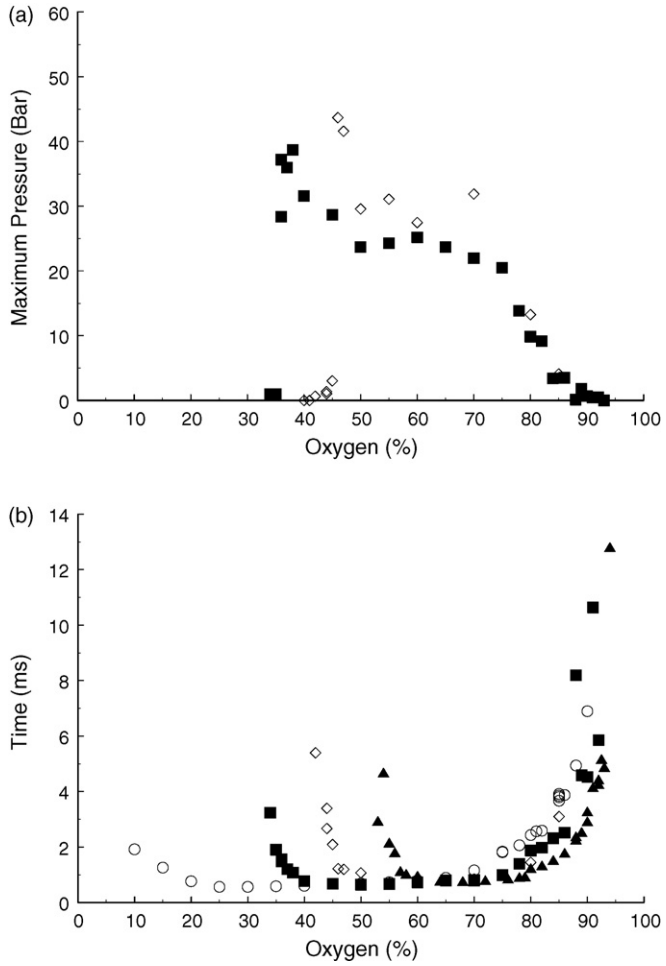

Fig. 8. Variation in (a) maximum pressure and (b) time to maximum pressure for various hydrogen–methane mixtures as a function of oxygen concentration. ○- H_2 ;■- 0.33 CH_4 + 0.67 H_2; ◊ - 0.67 CH_4 + 0.33 H_2 and ♦- CH_4.

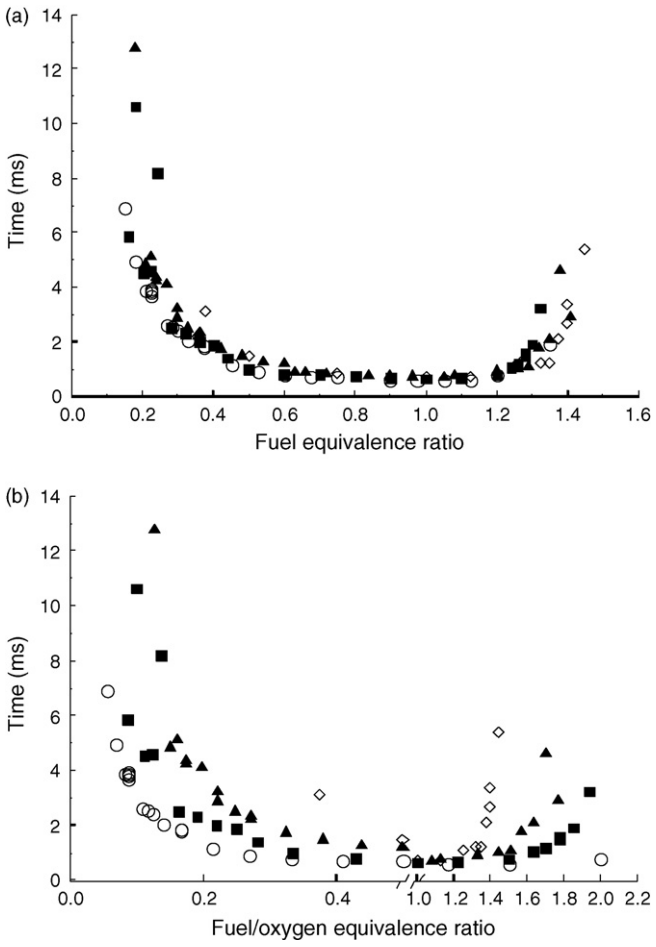

Fig. 9. Variation in time to maximum pressure for various hydrogen–methane mixtures as a function of equivalence ratios referenced to stoichiometric compositions based on a) fuel b) fuel/oxygen. ○- H_2 ;■– 0.33CH_4 + 0.67 H_2; ◊ - 0.67CH_4 + 0.33 H_2 and ♦- CH_4.

bars, of the present experimental detonation limit estimates as well as two horizontal lines corresponding to i) the tube diameter and ii) the value πD. From this plot it would appear that the limiting cell width for the present studies is less than the tube diameter D.

The influence of variations in initial temperature and pressure are most easily identified for fuel rich mixtures. Increasing temperature has a very small effect whereas a significant change in limiting oxygen concentration is obtained as the pressure increases from 1 to 7 bar.

7.2. Methane–hydrogen–oxygen

The limits of onset of detonation for the hydrogen-oxygen-methane mixtures may be estimated from the plots shown in Fig. 11. Here the maximum pressures are plotted as a function of oxygen concentration. Also included are the induction zone length estimates and the onsets of rapid increases in predicted lengths for fuel-lean and fuel-rich mixtures are in general agreement with the experimental limits. However, it is not as easy to be as precise when defining limits for oxygen rich mixtures. They are however in general agreement with those reported by Agafonov and Frolov [30]. Fig. 12 presents cell width estimates for the pure fuels, based on the induction zone data presented in Fig. 11(a and b). A multiplier, n, of 60 has been used in both instances as well as arbitrary values of $n = 10$ for methane and $n = 4$ for hydrogen. Also plotted on the figures (solid diamond symbol) are cell width measurement by Manzhalei et al. [37] and Aminallah et al. [38]. Reasonable agreement between measurement and prediction is obtained with hydrogen for $n = 60$, whereas better agreement in methane occurs for $n = 10$.

As the scheme presented by Tan [32] was not developed specifically for methane a further short series of induction zone length

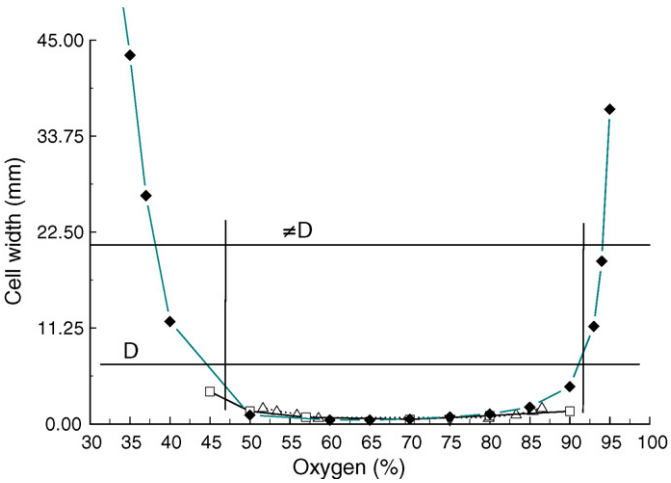

Fig. 10. Comparison of experimental detonation limits (vertical bars) with predicted (○- $60L_i$) and measured (▲) cell widths [25] for ethylene–oxygen.

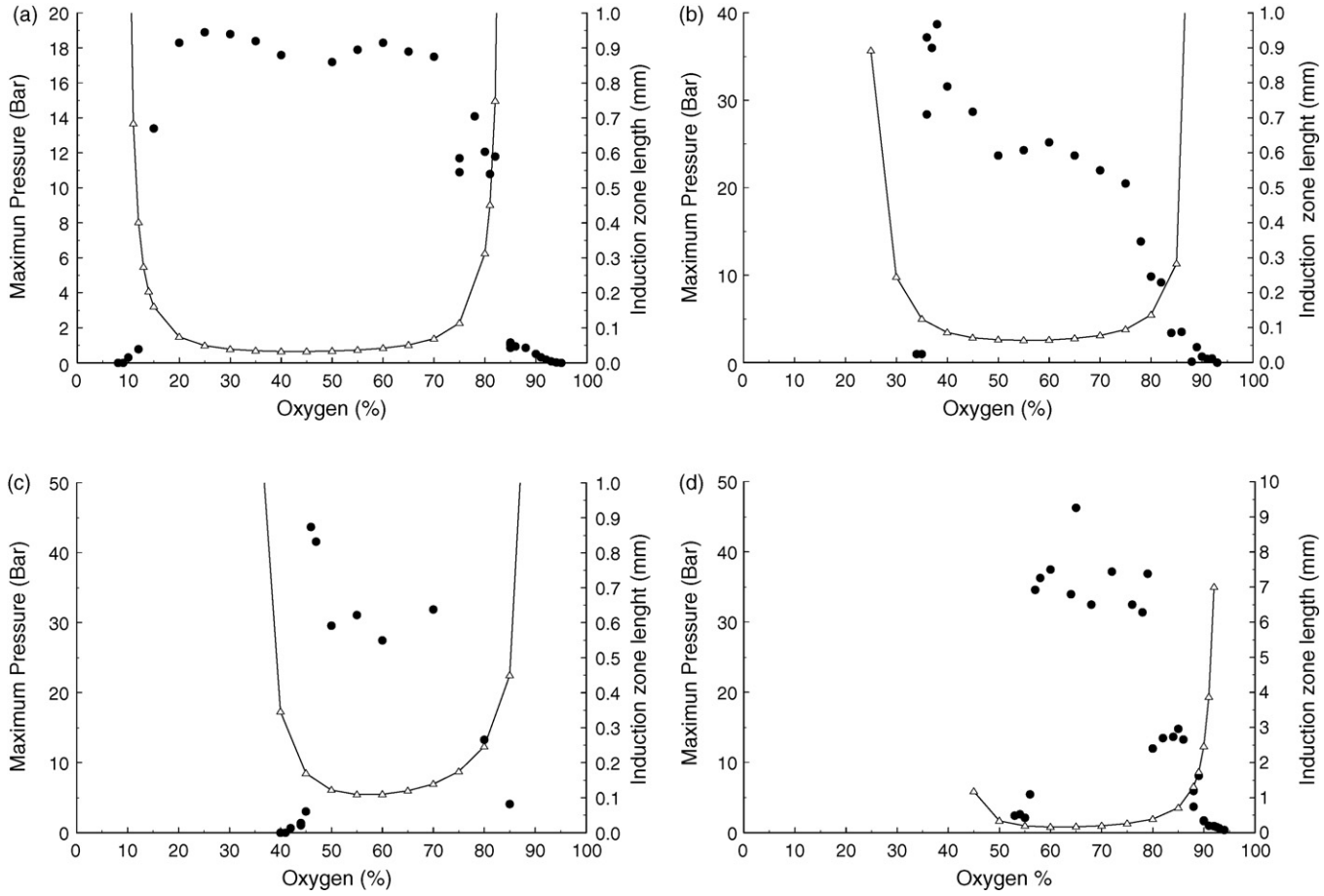

Fig. 11. Variations in maximum pressure(●)and computed induction zone length (△) for the following mixtures of methane and hydrogen with oxygen. (a) Pure H_2, (b) $0.33C_2H_4 + 0.67\ H_2$, (c) $0.67C_2H_4 + 0.33\ H_2$ and (d) pure CH_4.

calculations were undertaken using the latest version 3 of the GRIMech mechanism [39], which is optimised for high temperature natural gas ignition delay calculations. As can be seen from Fig. 12(b). There are some systematic differences between the absolute ignition delays predicted, by the two schemes, with the GRIM delays some 25% shorter than the values obtained using the Tan scheme. The use of $n = 10$ again provides a predicted cell width closer to the single experimental measurement available.

Finally, as with ethylene–oxygen the predicted cell size at the establishment limits appear to correlate better with a value less than the tube diameter D than a larger multiple of D.

7.3. Ethylene-air limits

Whilst the present studies are primarily concerned with fuel–oxygen mixtures, fuel-air mixtures are of equal interest. Recent observations of flame acceleration and transition to detonation in a 30 m long 150 mm diameter pipe have allowed detonation limits to be estimated, again with a 0.6 J spark source [40]. These limits are indicated by the vertical bars in Fig. 13. Also plotted on this figure are cell widths predicted during the present studies, using $n = 60$, and measured cell widths in ethylene-air. The establishment limits observed in a 30 m length of pipe are far narrower than limits obtained for cell widths of the order of the tube diameter. To match present observations a cell width some one third of the tube diameter is more appropriate. The experimental limits are also narrower than those reported in a 70 mm tube for a powerful initiation source, by Borisov and Loban [41] who observed limits of 3.3% and 14.7% in ethylene-air. These are to be compared with the limits in Fig. 15, which are of the order 6% to 9% in the 150 mm pipe.

Results have also been obtained recently in a 50 mm diameter tube, se Fig. 14. Here the limit of significant levels of overpressure development can be seen to correlate with detonation cell widths reported by Knystautas et al. [42].

7.4. Kinetics based cell computations and estimation of limits

It would seem from the above that induction zone calculations or direct cell size measurements can provide a useful means of correlating near limit behaviour in fuel–oxygen mixtures. The data however also indicates another important fact, the criterion that emerges from the present study for a low energy source, $\lambda \approx D/3$ is significantly different to that obtained in previous tests with a high energy source, $\pi D < \lambda < 2\pi D$. Thus, as smaller cells correspond to a more reactive mixtures, a more reactive mixture is required if detonation is to evolve from a low energy source than that required for a high energy source to initiate detonation directly.

Two limits may thus be defined. The first are propagation limits, beyond which it is not possible for a self-sustaining detonation to continue to propagate in a tube of particular cross-section. The second are establishment limits, that lie within the propagation limits, outside which detonation cannot evolve in the tube from a low energy source. The present data thus provides quantitative data on when detonations will or will not be *established*. As a consequence

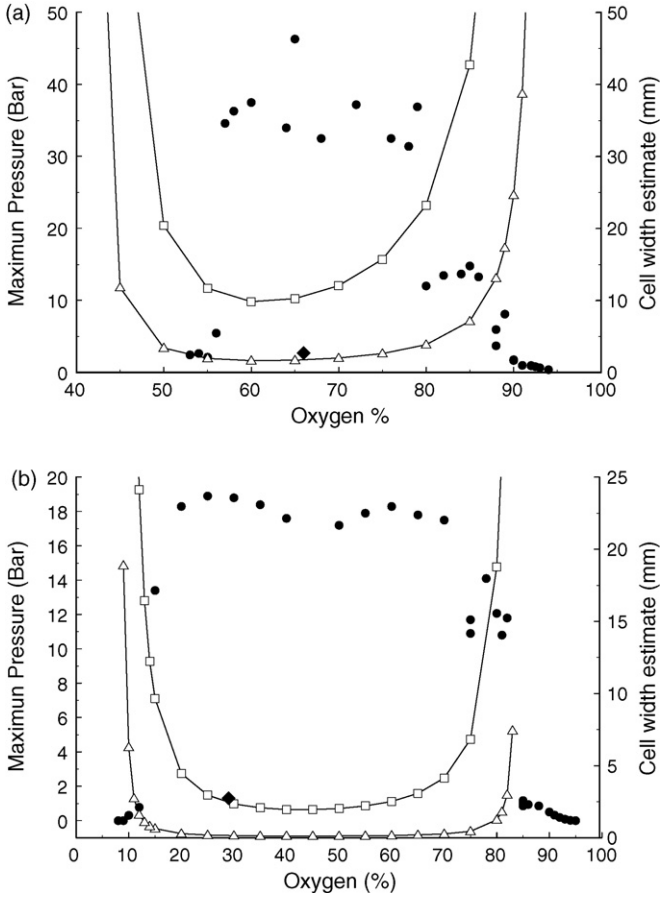

Fig. 12. Variations in maximum pressure (●) and estimated cell width based on computed induction zone length; a) methane-oxygen, △- $10L_i$, □- $60L_i$, dashed line – $10L_i$ based on GRIMech V3; b) hydrogen-oxygen. △- 4 L_i, □ - $60L_i$. ♦- measured cell width [32,33].

of these two limits, there are instances when detonation will not *evolve* from a low energy source even if the pipe geometry will *permit* a steady-state detonation to propagate in a self-sustained manner. The data is consistent with the studies of Dupré et al. [7,8] and Knystautas et al. [43] who obtained different propagation limits for different initiating mechanisms.

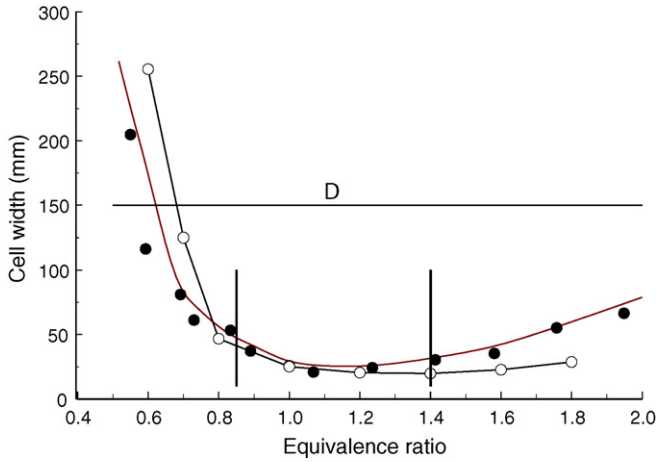

Fig. 13. Comparison of experimental detonation limits in a 150 mm diameter tube (vertical bars) with measured (●) and present predicted cell widths (◯- 60 L_i) for ethylene-air.

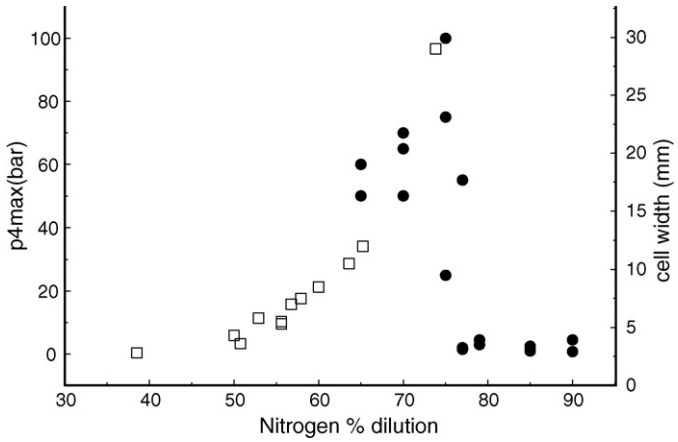

Fig. 14. Maximum overpressure observed in a 50 mm pipe together with measured values of detonation cell width reported by Knystautas et al. [43]; test gas mixture stoichiometric ethylene–oxygen with added nitrogen.

One should also treat propagation detonation limits from very high energy sources with care, for example those reported by Kogarko [44] in a tube of 3.76 m and diameter 305 mm are valid when the initiation source is a 70 g high explosive charge. This is linked to the issue of whether a detonation will be sustained indefinitely after transition occurs. Recent unpublished results [40] indicate that a limiting diameter closer to the cell size is a more appropriate propagation for long pipes, based on the velocity distance histories of directly initiated detonations ethylene- and propane-air in a 40 m long 80 mm pipe. As can be seen in Fig. 14, the propane-air mixture appears to decay slowly along the length of the tube. The velocity of the ethylene-air mixture on the other hand tends to a constant value some 1.5% below the theoretical CJ value.

Our general findings confirm the conclusions of Dupré et al. [45], that cell size data provides a good basis for correlating limit behaviour in detonations. The factors to be included in any general analysis are mixture chemical reactivity, geometrical dimension and source ignition energy. In practice, theoretical predictions of cell size rely on the availability of chemical kinetic schemes. Thus, whilst potentially useful, the applicability of the approach to mixtures that differ from those routinely studied in research laboratories is, at present, still very limited. The same is true of predictions based on direct detonation cell size measurements.

The results however also suggest that there is no universal correlation of induction zone length and cell size. It may be that this is due to the differing regularity of the cell structure between different fuels. Moen et al. [46] have reported that detonations with regular uniform patterned cells are more easily attenuated than those with irregular patterns.

Finally, there is the question of which limit should be used in any practical assessment. The establishment limit is attractive, as it provides an indication of an inability to undergo transition to detonation however, in practice, the propagation limits are more conservative.

8. Methane–ammonia–oxygen

8.1. Experimental details

Experiments were performed in the same 7 mm diameter stainless steel tube but in this case the test gas mixtures were first prepared in a separate vessel by the method of partial pressures at ambient temperature after which they were introduced into the

previously evacuated 7 mm tube as a required. Mixture ignition was attempted using a high energy spark.

Ignition and flame propagation was monitored by two high temperature Kistler gauges and a photodiode. A photodiode was located 0.63 m from the ignition end of the tube and was used to define successful flame propagation along the tube. The Kistler gauges were located 0.696 and 946 m from the ignition end.

8.2. Experimental results

A total of 122 tests were conducted and the experimental parameters investigated were the initial gas pressure, temperature and composition. Compositional ranges were obtained by varying the oxygen content whilst maintaining the methane/ammonia ratio constant at CH_4/NH_3 1.0:1.176.

The experimental pressure and photodiode data obtained allowed several combustion regimes to be identified:

- No ignition (no pressure or light emission),
- Ignition followed by quenching (pressure but no emission at photodiode location),
- Flame propagation (pressure and emission at photodiode),
- Transition to detonation.

Fig. 15 presents a composite plot summarising the variation in combustion modes observed as a function of oxygen content and initial test pressure, in this case for an initial temperature of 200. A similar plot, in this case showing the effect of increasing temperature is shown in Fig. 16. The corresponding oxygen concentrations in the test mixtures are listed in Table 1.

The average flame speeds measured during tests where continuous flame propagation was observed are given in Figs. 17 and 18. In general the measured flame speeds were modest for all mixtures where the oxygen percentage was 39% or less.

Similarly, violent pressure transients were not observed for mixtures with an oxygen concentration below 40%. Beyond this critical oxygen concentration detonation sometimes developed, especially for initial pressures above ambient.

8.3. Detonation-cell with predictions

Detonation-cell with predictions was undertaken using the same method as described above. The constant, *n*, used to relate

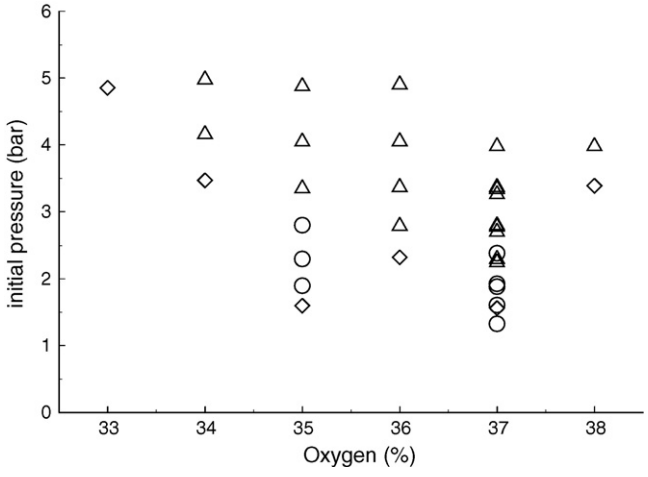

Fig. 15. Flame propagation modes for various methane-ammonia-oxygen mixtures and initial pressures. Initial temperatures 200 °C. △- flame propagation; ◯- flame quenched; ◊ - no ignition.

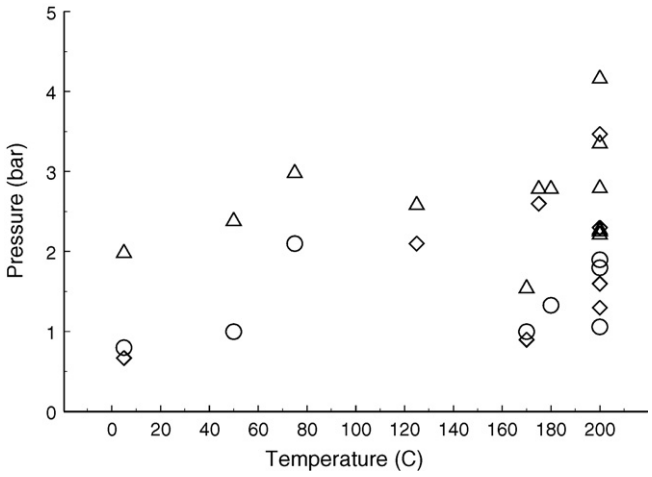

Fig. 16. Flame propagation modes versus initial temperature for various methane-ammonia-oxygen mixtures; Oxygen % varies; see Table 1: △- flame propagation; ◯- flame quenched; ◊ - no ignition.

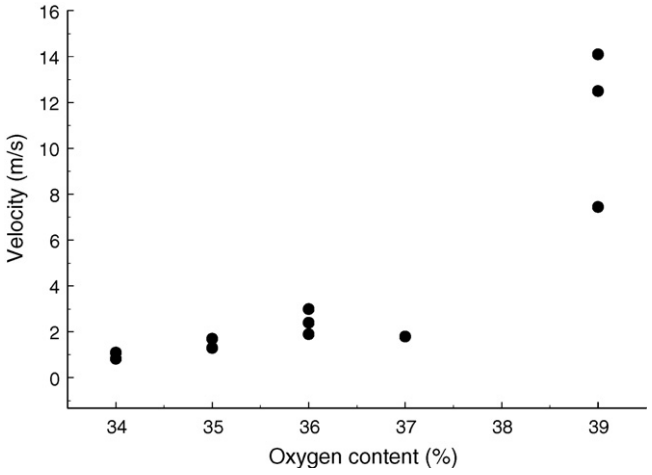

Fig. 17. Measured average flame speeds as function of oxygen content: initial pressure 1 bar?; Initial temperature 200 °C.

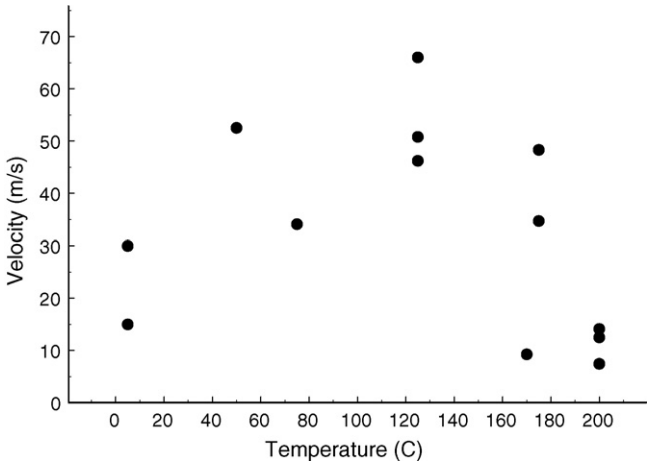

Fig. 18. Measured average flame speeds as function of oxygen content: initial pressure 1 bar; Initial temperature 200 °C.

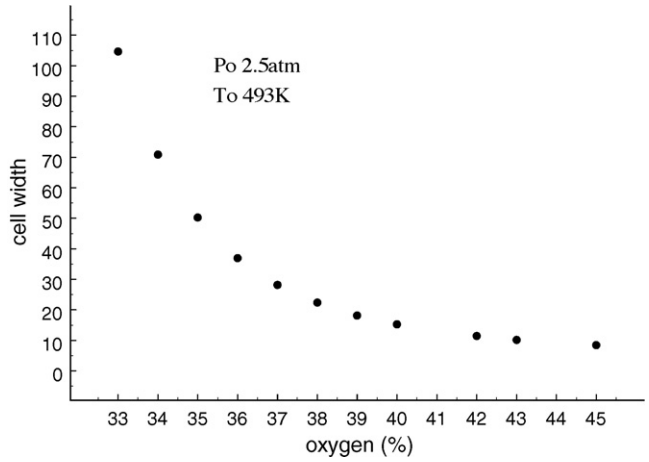

Fig. 19. Variation in predicted detonation cell width as a function of oxygen content; Initial temperature 200 °C, initial pressure; 2.5 atmosphere.

the estimated induction zone length L_i to the cell width λ was again taken as 60.

Calculated cell widths as a function of oxygen concentration for an initial temperature of 200 °C and an initial pressure of 2.5 atmospheres are given in Fig. 19 and it is interesting to note that the boundary separating slow flames and more violent events, described above observed at an oxygen concentration of around 39–40% for an initial temperature of 200 °C corresponds in these predictions to a detonation cell width of *ca*. 22 mm, i.e. circa πD.

Fig. 20 shows the predicted cell width variation with increasing initial pressure for an initial temperature of 200 °C and an oxygen concentration of 35%. In this case a critical cell width of 22 mm would only appear to be predicted for initial pressures greater than 5 atmospheres.

Similarly, Fig. 21 shows the predicted cell width variation with increasing initial pressure for an initial temperature of 5 °C and an oxygen concentration of 39%.

As described above, detonation events were only observed for oxygen concentrations in excess of 39%. The combinations of initial pressure and oxygen concentrations where detonation was observed to develop are summarised in Fig. 22, obtained for tests at an initial temperature of 5 °C. Also presented on this figure are the corresponding predicted detonation cell widths at an initial temperature of 5 °C and an initial pressure of 1 atmosphere. Again the variation in cell size with oxygen concentration reflects qualitatively changes in the different modes of combustion observed in the experimental tests.

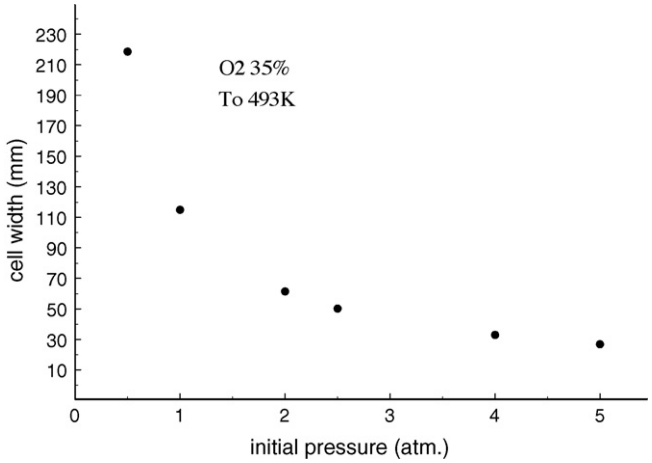

Fig. 20. Variation in predicted detonation cell width as a function of initial pressure: oxygen content 35%; Initial temperature 200 °C.

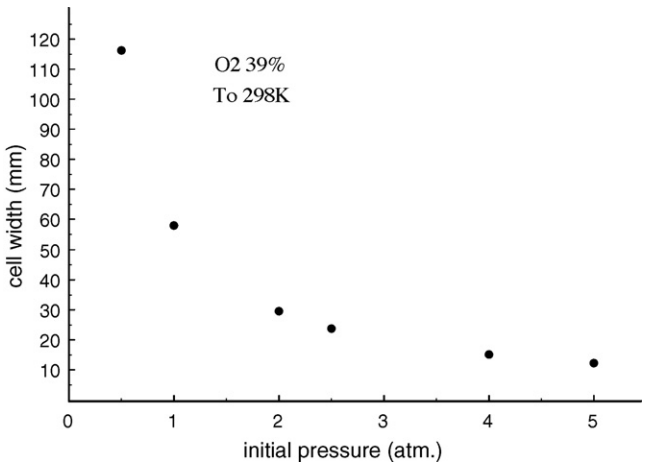

Fig. 21. Variation in predicted detonation cell width as a function of initial pressure: oxygen content 39%; Initial temperature 5 °C.

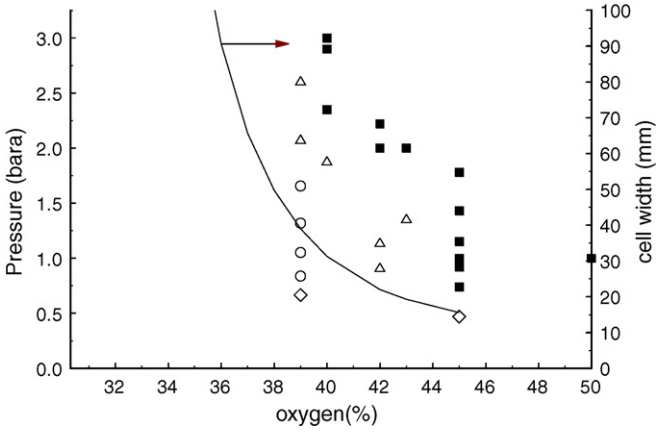

Fig. 22. Flame propagation modes observed for various mixtures and initial pressures. Initial temperature 5 °C. △- Flame propagation; ○- flame quenched; ◊ - no ignition; ■- detonation. Solid line – predicted detonation cell widths.

9. Summary of conclusions

The limiting minimum oxygen concentration in ethylene for which flame propagation was observed in a 7 mm stainless steel pipe decreased from 40% to 26% as the initial pressure was increased from 1 to 7 bar absolute. The corresponding limits for the establishment of detonation are less clearly defined but the limiting oxygen concentration decreased from *ca.* 46% to 36% as the pressure was increased from 1 bar to 7 bar. Increasing temperature had significantly less effect on this fuel rich limit. At the fuel lean limit neither increasing temperature or pressure has any significant effect on the observed limit of establishment of detonation.

Kinetic predictions of induction zone length correlate well with measured cell sizes, using a multiplication factor of 60 for ethylene- and hydrogen decreasing to 10 for methane-oxygen. These are in reasonably argument with the present limits for the establishment of detonation, where a limit criterion of cell width $\lambda \approx D/3$, where D is the pipe diameter, appears more appropriate for low energy ignition sources. This was observed for fuel–oxygen mixtures at elevated temperatures and pressures in a 7 mm diameter tube as well as in ethylene-air at atmospheric pressure and temperature

in a 150 mm diameter pipe. Given the errors inherent in kinetic predictions and cell size measurements (which can be several hundred percent) it is concluded that a cell length of the order of the tube diameter is the most appropriate as an initial practical scoping parameter.

Although no published cell size data is available against which to validate the cell width predictions for the methane–ammonia–oxygen mixtures tested, the predicted cell widths correlated well with be observed ignition and flame propagation modes.

Overall the results with all mixtures indicate that whilst detonation cell widths do not provide a quantitative measure of the conditions for which detonation may develop in a pipe of given diameter, for prescribed initial conditions, detonation cell size data does provide useful qualitative guidance, particularly if preliminary experimental safety tests are to be undertaken.

Acknowledgements

The studies reported were initially undertaken whilst the author was affiliated with the Shock and Detonation Physics Research Group at the University of Wales Aberystwyth UK.

Financial support for the work was provided variously from the following: Shell Research, the Pipe*Ex* consortium (BNFL, BP, DSM Research Netherlands, ICI and UK HSE).

The views expressed in the paper are those of the author and do not necessarily represent the views of the sponsors. Technical input provided by Gwyn Oakley and Paul Clarke whilst developing and undertaking the experimental work is gratefully acknowledged.

References

[1] J.J. Erpenbeck, Fluid Phys. 7 (1964) 684–696.
[2] D.S. Stewart, Twenty-Seventh Symposium. (International) on Combustion, Combustion Institute, Pittsburgh, Pa, 1998, pp. 2189–2205.
[3] D.S. Stewart, Twenty-Sixth Symposium. (International) on Combustion, Combustion Institute, Pittsburgh, Pa, 1996, pp. 2981–2989.
[4] M.A. Nettleton, Gaseous Detonations: Their Nature, Effects and Control, Chapman & Hall, 1987.
[5] R.A. Strehlow, Fundamentals of Combustion, International Textbook Company, 1968.
[6] D.H. Edwards, G. Hooper, D.J. Parry, Acta Astronautica 15 (1970) 323–333.
[7] G. Dupré, R. Knustautas, J.H. Lee, AIAA, Prog. Astronaut. Aeronaut. 106 (1985) 244–259.
[8] G. Dupré, O. Peraldi, J. Joannon, J.H. Lee, R. Knustautas, AIAA, Prog. Astronaut. Aeronaut. 133 (1990) 156–169.
[9] I.O. Moen, M. Donato, R. Knystautas, J.H. Lee, Eighteenth Symposium. (International) on Combustion, Combustion Institute, Pittsburgh, Pa, 1990, pp. 1615–1622.
[10] L.E. Bollinger, M.C. Fong, R. Edse, ARS (1961) 588–595.
[11] L.E. Bollinger, AIAA J. 2 (1) (1964) 131–133.
[12] L.E. Bollinger, AIAA J. 4 (10) (1996) 1773–1776.
[13] I. Ginsburgh, W.L. Buckley, Chem. Eng. Prog. 1 (1963) 75–85.
[14] V.A. Popov, Seventh Symposium. (International) on Combustion, Combustion Institute, Pittsburgh, Pa, 1958, pp. 799–806.
[15] A.V. Bunev, Combust. Explosion Shock Waves 8 (1974) 67–69.
[16] Y.N. Shebeko, S.G. Tsarichenko, A.V. Trunev, A.Y. Kaplin, A.A. Zaitsev, Combust. Explosion Shock Waves 30 (1993) 15–18.
[17] Chapin, D., Tangirala, V., Dean, A., Ignition and detonation initiation of moving hydrogen-air mixtures at elevated temperature and pressure, Paper presented at 45th AIAA Aerospace Sciences Meeting and Exhibit, Reno, Nevada, January 8–11, AIAA-2007-236, 2007.
[18] J. Card, D. Rival, G. Giccarelli, DDT in fuel-air mixtures at elevated temperatures and pressures, Shock Waves 14 (3) (2005) 167–173.
[19] P. Bauer, H.N. Presles, M. Dunand, AIAA Prog. Astronaut. Aeronaut. 133 (1990) 56–62.
[20] P.A. Bauer, H.N. Presles, P.J. Heuze, J.C. Boden, AIAA, Prog. Astronaut. Aeronaut. 106 (1986) 321–328.
[21] F.M. Belles, Seventh Symposium (International) on Combustion, Combustion Institute, Pittsburgh, Pa, 1958, pp. 745–751.
[22] C. Westbrook, P. Urtiew, Combust. Explosion Shock Waves 19 (1983) 753–766.
[23] C. Westbrook, P. Urtiew, Nineteenth Symposium (International) on Combustion, Combustion Institute, Pittsburgh, Pa, 1982, pp. 615–623.
[24] R.A. Strehlow, D.C. Engel, AIIA J. 7 (1969) 492–496.
[25] R.A. Strehlow, D.C. Engel, AIIA J. 7 (1969) 487–491.
[26] D.C. Bull, J.E. Elsworth, P.J. Shuff, E. Metcalf, Combust. Flame 45 (1982) 7–22.
[27] C.M. Bradley, A kinetic approach to detonation in gaseous hydrogen- and hydrocarbon-oxygen systems, Ph.D. Thesis, Imperial College of Science and Technology, London, 1997.
[28] A.I. Gavrikov, A.A. Efimenkov, S.B. Dorefeev, A model for detonation cell size prediction from chemical kinetics, Combust. Flame 120 (2000) 19–33.
[29] Y. Auffret, D. Desbordes, H.N. Presles, Detonation structure and detonability of C_2H_2–O_2 mixtures at elevated initial temperature, Shock Waves 11 (2001) 89–96.
[30] G.L. Agafonov, S.M. Frolov, Combust. Explosion Shock Waves 30 (1994) 91–100.
[31] H.D. Ng, Y. Ju, J.H.S. Lee, Assessment of detonation hazards in high pressure hydrogen storage from chemical sensitivity analysis, Int. J. Hydrogen Energy 32 (2007) 93–99.
[32] Y. Tan, Cinétique de combustion du gaz naturel: étude expérimentale et modélisation. Thése, Université de Pirerre et Marie Curie, Paris VI, Juliet, 1994.
[33] A. Makris, J.H.S. Lee, R. Knystautas, Twenty-Fifth Symposium. (International) on Combustion, Combustion Institute, Pittsburgh, Pa, 1994, pp. 65–71.
[34] I.O. Moen, S.B. Murray, D. Bjerkedvedt, A. Rinnan, R. Knystautas, J.H.S. Lee, Nineteenth Symposium (International) on Combustion, Combustion Institute, Pittsburgh, 1982, pp. 5635–5644.
[35] H.Gg Wagner, A. Ferri, Fundamental data obtained from shock tube experiments, in: AGARDograpgh No. 41, Pergamon Press, 1961.
[36] W. Pusch, H.Gg Wagner, Ber. Bunsenges. Phys Chem. 69 (1964) 503.
[37] V.I. Manzhalei, V.V. Mitrofanov, V.A. Subbotin, Combust. Explosion Shock Waves 10 (1974) 89–95.
[38] M. Aminallah, J. Brossard, A. Vasiliev, Prog. Astronaut. Aeronaut. 153 (1993) 203–228.
[39] G.P. Smith, D.M. Golden, M. Frenklach, N.W. Moriarty, B. Eiteneer, M. Goldenberg, C.T. Bowman, R.K Hanson, S. Song, W.C. Gardiner, V.L. Lissianski, Z. Qin, http://www.me.berkeley.edu/gri_mech/.
[40] G.O. Thomas, N.S. Lamoureux, G.L. Oakley, Experimental Studies of Flame Acceleration and DDT in Pipes, Confidential Report UWA/Pipe*Ex*/R210399, University of Wales, Aberystwyth UK, March 1999.
[41] A.A. Borisov, S.A. Loban, Combust. Explosion Shock Waves 13 (1977) 618–621.
[42] R. Knystautas, J.H. Lee, C.M. Guirao, The critical tube diameter for detonation failure in hydrocarbon-air mixtures, Combust. Flame 48 (1) (1982) 63–83.
[43] R. Knystautas, J.H. Lee, O. Peraldi, AIAA Progress Astronautics Aeronautics 106 (1986) 66–89.
[44] S.M. Kogarko, Sov. Phys. Tech. Phys. 28 (1958), 1904:1916.
[45] G. Dupré, J. Joannon, R. Knystautas, J.H.S. Lee, Twentythird Symposium (International) on Combustion, Combustion Institute, Pittsburgh, Pa, 1990, pp. 1813–1820.
[46] I.O. Moen, A. Sulmistras, G.O. Thomas, D. Bjerkedvedt, P. Thibault, Dynamics of Explosions AIAA Progress in Astronautics and Aeronautics, vol. 106, 1986, pp. 220–243.